J|A|C|S COMMUNICATIONS

Published on Web 08/23/2010

Identification of Bacteria by Conjugated Oligoelectrolyte/Single-Stranded DNA Electrostatic Complexes

Aidee Duarte,[†] Arkadiusz Chworos,[†] Suvi F. Flagan,[‡] Grady Hanrahan,[§] and Guillermo C. Bazan*,[†]

Department of Chemistry & Biochemistry, Department of Materials, Center for Polymers and Organic Solids, and Marine Science Institute, University of California, Santa Barbara, California 93106, and Department of Chemistry, California Lutheran University, Thousand Oaks, California 91360

Received June 29, 2010; E-mail: bazan@chem.ucsb.edu

Abstract: Electrostatic complexes containing a cationic conjugated oligoelectrolyte (COE) and fluorescein (FAM)-labeled single-stranded DNA (ssDNA) serve as the basis for identifying various bacteria. The approach involves the preparation of five COE/ssDNA$_x$-FAM electrostatic complexes, which differ in the ssDNA composition and which provide different photoluminescence (PL) spectra as a result of different degrees of energy transfer efficiency from the COE to FAM. Changes in the PL spectra upon addition of the bacteria can be quantified, and the differential response from the five ssDNAs gives rise to a multicomponent array response that allows identification of the microorganism under investigation.

Bacterial identification is of interest due to the numerous species associated with infectious diseases and of relevance in biological warfare.[1] In the United States alone, food-borne diseases cause approximately 76 million illnesses and 5000 deaths each year, with 30% and 70%, respectively, stemming from bacterial pathogens.[1a] Typical methods for identifying bacteria include culturing in selective media, visual analysis of morphological structure, and examination of immunological characteristics.[2] These techniques necessitate trained microbiologists. Efficient identification protocols that may be automated therefore remain an important priority in health care, food safety, environmental applications, and homeland security.

Conjugated polyelectrolytes (CPEs) have an electronically delocalized backbone with pendant groups bearing ionic functionalities.[3] These materials, together with their related conjugated oligoelectrolytes (COEs), have been incorporated into optical biosensory assays.[4] The charged pendant groups yield the opportunity to form electrostatic aggregates, i.e., coacervates, with oppositely charged macromolecules.[5] The complementary macromolecule can be designed to act as an emission quencher or to participate in Förster resonance energy transfer (FRET). The latter approach has been successfully implemented in protein identification by using an array of nanoaggregates comprised of cationic COE and dye-labeled single-stranded DNA (ssDNA).[4a] Optical changes are caused by structural modifications within the aggregate from nonspecific interactions with the proteins. It is worth mentioning that the original concept for taking advantage of the optical properties of CPEs in array-type identification of proteins and microorganisms arises from work by Bunz and Rotello with composites containing oppositely charged metal nanoparticles.[4i−k]

Scheme 1. Molecular Structure of FPF and ssDNA$_x$-FAM Sequences

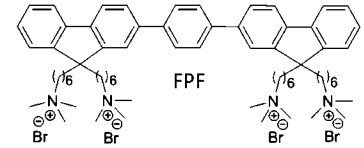

ssDNA$_1$-FAM 5′-FAM-ATC TTG ACT ATG TGG GTG CT
ssDNA$_2$-FAM 5′-FAM-AGC ACC CAC ATA GTC AAG AT
ssDNA$_3$-FAM 5′-FAM-AAA AAA AAA AAA AAA AAA AA
ssDNA$_4$-FAM 5′-FAM-CCC CCC CCC CCC CCC CCC CC
ssDNA$_5$-FAM 5′-FAM-TTT TTT TTT TTT TTT TTT TT

Herein we show that electrostatic complexes built from a tetracationic COE and ssDNA serve as the basis for identifying bacteria. Specifically, we employ FPF as the FRET donor with fluorescein (FAM)-labeled ssDNAs as the acceptors, as depicted in Scheme 1. The five different FPF + ssDNA$_x$-FAM ($x = 1-5$) combinations constitute the responsive array. From preliminary studies, a charge ratio of $R_{-/+} = 1.2$ was chosen as it produced the most stable and reproducible photoluminescence (PL) spectra (Supporting Information). Excitation at 336 nm, where FPF predominantly absorbs, produces a PL spectrum comprised of the FPF emission (365−480 nm) and sensitized FAM emission (490−600 nm); see Figure 1 for the example utilizing ssDNA$_1$-FAM. Gram-negative (*Escherichia coli* K12, *Escherichia coli* FAD-1, *Sporomusa* DMG58) and gram-positive (*Lactobacillus acidophilus*, *Rhodopseudomonas palustris* CGA009, *Streptococcus mutans*) bacteria were targeted in this investigation.

Briefly, the probes were prepared by mixing the COE and the ssDNA$_x$-FAM in phosphate buffer. Aliquots were introduced into a 96-well plate, where the initial spectra were recorded. Bacteria were separated from the growth media and resuspended in phosphate buffer to achieve an optical density (OD) of 1.0 at 600 nm. The bacteria solutions were added to each probe up to a final concentration corresponding to an OD of 0.05. PL spectra were

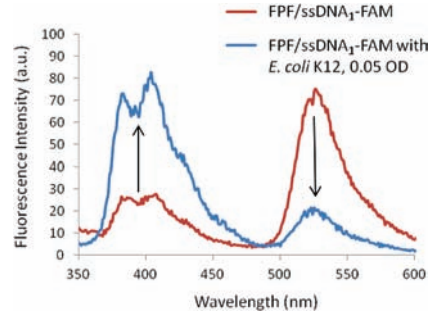

Figure 1. Initial PL spectra (red) of the FPF/ssDNA$_1$-FAM complex and final spectra (blue) after the addition of *Escherichia coli* K12. The excitation wavelength was 336 nm.

[†] Department of Chemistry & Biochemistry, Department of Materials, Center for Polymers and Organic Solids, University of California, Santa Barbara.
[‡] Marine Science Institute, University of California, Santa Barbara.
[§] Department of Chemistry, California Lutheran University.

10.1021/ja105747b

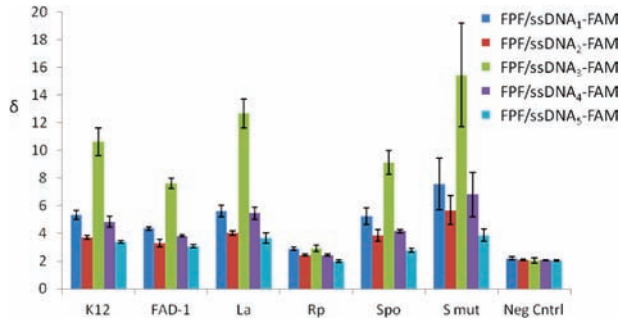

Figure 2. Complete response array to six different bacteria: K12, *Escherichia coli* K12; FAD-1, *Escherichia coli* FAD-1; La, *Lactobacillus acidophilus*; Rp, *Rhodopseudomonas palustris* CGA009; Spo, *Sporomusa* DMG58; S mut, *Streptococcus mutans*; Neg Cntrl, negative phosphate buffer control. Error bars represent 3σ.

recorded after 15 min interaction time. To ensure that statistical variations due to gross, systematic, and random errors are taken into account, independent probe and bacteria solutions were prepared for each measurement discussed below.

Addition of the bacteria solutions changes the PL spectra from the FPF/ssDNA$_x$-FAM aggregates; a typical example is shown in Figure 1 using FPF/ssDNA$_1$-FAM. One observes that the FPF emission typically increases, while the sensitized FAM emission decreases. This change implies a structural modification within the nanoaggregates as a result of nonspecific interactions with the bacterial surface. The decrease in the sensitized FAM emission and the increase in FPF emission suggest an increase in the average distance between the FRET donor−acceptor pair.

Our approach begins by individually exposing the five distinct electrostatic aggregates (i.e., FPF/ssDNA$_x$-FAM, $x = 1-5$) to the bacteria. Changes in the PL spectra can be quantified by the parameter δ, as defined in eq 1:

$$\delta = \frac{B_f}{B_i} + \frac{G_i}{G_f} \tag{1}$$

where B_i and B_f are the initial and final FPF emissions integrated between 370 and 450 nm, before and after bacteria addition, respectively; G_i and G_f are the corresponding FAM emissions integrated between 500 and 590 nm. The collective δ response from the five independent aggregates creates a signature pattern for each bacterium. Figure 2 provides a complete summary of the composite δ responses. It is reasonable that there are various other ways to process the PL spectra; however, we found that δ in eq 1 yields a simple method that provides consistently distinct patterns. The lowest δ values are obtained for *R. palustris*, possibly due to the lower number of cells introduced. *R. palustris* is a purple bacterium, and its red color contributes to loss in transmittance at 600 nm used to measure cell abundance; consequently, there are a lower number of cells at 1.0 OD than for the other bacteria. The negative control, 10 μL of phosphate buffer, is included in Figure 2 to demonstrate that the *R. palustris* pattern is statistically different from the negative control.

A regularized discriminant analysis (RDA) algorithm, given by

$$d_k(\mathbf{X}) = (\mathbf{X} - \boldsymbol{\mu}_k)^T \sum_k^{-1}(\lambda,\gamma)(\mathbf{X} - \boldsymbol{\mu}_k) + \ln\left|\sum_k(\lambda,\gamma)\right| - 2\ln\pi_k \tag{2}$$

was applied for the δ pattern classification. The formal purpose of discriminant analysis is to assign objects to one of several classes on the basis of a set of measurements $\mathbf{X} = (X_1, X_2, ..., X_n)$ obtained

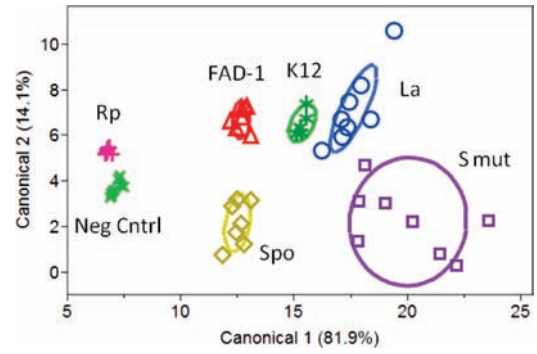

Figure 3. Canonical score plot of the response pattern. Ellipses represent the 95% confidence limits for each mean.

from each observation.[6] During the regularization process, the bias and variance trade-off is regulated by two user-defined parameters, λ and γ, which control the degree of shrinkage of the individual class covariance matrix and modify covariances across variables, respectively. For this study, λ and γ were set at 0.5 and 0.0, respectively, to improve parameter estimates by biasing them away from their sample-based values.

Bacterial classifications are made on the basis of the shortest Mahalanobis distances from each point to each class's multivariate mean.[7] Canonicals 1−5 contained 81.9%, 14.1%, 2.4%, 1.5%, and 0.1% of the variability, respectively. Figure 3 shows the canonical plot with the first two scores. Each of the bacteria formed their own clusters in the two-dimensional space with no overlapping 95% confidence ellipses. Additionally, there were no reported model misclassifications of the bacteria. Moreover, the −2 log likelihood value of 0.01 indicates that the model is a good fit for the experimental data.

In summary, we report the successful implementation of FPF/ssDNA$_x$-FAM electrostatic complexes for bacterial identification. This technique benefits from readily available molecules with precisely determined structures and may be relevant in situations where microbiologists are not available to identify specific strains and bacterial detection is important to prevent disease propagation and ensure water and food quality. From a practical perspective, we recognize that array-based detection methods are challenged when confronted with large variations in concentration and in situations where a mixture of targets is present in the sample.[8] That individual bacteria colonies can be easily obtained and that the quantity of bacteria can be arbitrarily controlled by simple examination of the OD may provide a competitive advantage relative to molecular targets.

Acknowledgment. We thank the Institute for Collaborative Biotechnologies (contract no. W911NF-09-D-0001 from the U.S. Army Research Office), the National Science Foundation (68-A-1084096), and The National Academies, Ford Foundation Diversity Fellowship, for financial support.

Supporting Information Available: Experimental procedures, UV absorption and photoluminescence spectra of FPF and ssDNA$_x$-FAM, as well as PL spectra for $R_{-/+} = 1.0$ and 1.2 aggregates after addition of *E. coli* K12. This material is available free of charge via the Internet at http://pubs.acs.org.

References

(1) (a) Mead, P. S.; Slutsker, L.; Dietz, V.; McCaig, L. F.; Bresee, J. S.; Shapiro, C.; Griffin, P. M.; Tauxe, R. V. *Emerging Infect. Dis.* **1999**, *5*, 607–625. (b) Ivnitski, D.; Abdel-Hamid, I.; Atanasov, P.; Wilkins, E. *Biosens. Bioelectron.* **1999**, *14*, 599–624. (c) Swaminathan, B.; Feng, P. *Annu. Rev. Microbiol.* **1994**, *48*, 401–426. (d) Baeumner, A. J.; Cohen, R. N.; Miksic, V.; Min, J.

Biosens. Bioelectron. **2003**, *18*, 405–413. (e) Gannon, J. C. *The Global Infectious Disease Threat and Its Implications for the United States*, NIE 99-17D; National Intelligence Council: Washington, DC, 2000; http://www.dni.gov/nic/PDF_GIF_otherprod/infectiousdisease/infectiousdiseases.pdf.

(2) (a) Reisner, B. S.; Woods, G. L. *J. Clin. Microbiol.* **1999**, *37*, 2024–2026. (b) Pommerville, J. C. *Alcamo's fundamentals of microbiology: Body systems*; Jones and Bartlett Publishers, LLC: Sudbury, 2010; pp 81−90.

(3) (a) Liu, B.; Bazan, G. C. *J. Am. Chem. Soc.* **2006**, *128*, 1188–1196. (b) Abbel, R.; Schenning, A. P. H. J.; Meijer, E. W. *J. Polym. Sci., Part A: Polym. Chem.* **2009**, *47*, 4215–4233.

(4) (a) Li, H.; Bazan, G. C. *Adv. Mater.* **2009**, *21*, 964–967. (b) Wang, D.; Gong, X.; Heeger, P. S.; Brininsland, F.; Bazan, G. C.; Heeger, A. J. *Proc. Natl. Acad. Sci. U.S.A.* **2001**, *99*, 49–53. (c) Jiang, H.; Taranekar, P.; Reynolds, J. R.; Schanze, K. S. *Angew. Chem., Int. Ed.* **2008**, *48*, 4300–4316. (d) Ho, H. A.; Najari, A.; Leclerc, M. *Acc. Chem. Res.* **2008**, *41*, 168–178. (e) Gaylord, B. S.; Heeger, A. J.; Bazan, G. C. *Proc. Natl. Acad. Sci. U.S.A.* **2002**, *99*, 10954–10957. (f) Liu, B.; Bazan, G. C. *Chem. Mater.* **2004**, *16*, 4467–4476. (g) Pu, K. Y.; Liu, B. *Macromolecules* **2008**, *41*, 6636–6640. (h) Xing, C.; Xu, Q.; Tang, H.; Liu, L.; Wang, S. *J. Am. Chem. Soc.* **2009**, *131*, 13117–13124. (i) You, C. C.; Miranda, O. R.; Gider, B.; Ghosh, P. S.; Kim, I.-B.; Erdogan, B.; Krovi, S. A.; Bunz, U. H. F.; Rotello, V. M. *Nat. Nanotechnol.* **2007**, *2*, 318–323. (j) Bunz, U. H. F.; Rotello, Vincent, M. *Angew. Chem., Int. Ed.* **2010**, *49*, 3268–3279. (k) Phillips, R. L.; Miranda, O. R.; You, C. C.; Rotello, V. M.; Bunz, U. H. F. *Angew. Chem., Int. Ed.* **2008**, *47*, 2590–2594.

(5) (a) Chi, C.; Chworos, A.; Zhang, J.; Mikhailovsky, A.; Bazan, G. C. *Adv. Funct. Mater.* **2008**, *18*, 3606–3612. (b) Aberem, M. B.; Najari, A.; Ho, H. A.; Gravel, J. F.; Nobert, P.; Boudreau, D.; Leclerc, M. *Adv. Mater.* **2006**, *18*, 2703–2707.

(6) (a) Friedman, J. H. *J. Am. Stat. Assoc.* **1989**, *84*, 165–175. (b) Vaid, T. P.; Burl, M. C.; Lewis, N. S. *Anal. Chem.* **2001**, *73*, 321–331. (c) Rao, R. K.; Tun, K.; Lakshminarayanan, S. *Ind. Eng. Chem. Res.* **2009**, *48*, 4899–4907.

(7) Bajaj, A.; Miranda, O. R.; Phillips, R.; Kim, I.-B.; Jerry, D. J.; Bunz, U. H. F.; Rotello, V. M. *J. Am. Chem. Soc.* **2009**, *132*, 1018–1022.

(8) Albert, K. J.; Lewis, N. S.; Schauer, C. L.; Sotzing, G. A.; Stitzel, S. E.; Vaid, T. P.; Walt, D. R. *Chem. Rev.* **2000**, *100*, 2595–2626.

JA105747B